Spinodal Dewetting of Thin Polymer Films

R. Xie,[1,2] A. Karim,[2,*] J. F. Douglas,[2,*] C. C. Han,[2] and R. A. Weiss[1]
[1]*Polymer Science Program and Department of Chemical Engineering, University of Connecticut, Storrs, Connecticut 06269*
[2]*Polymers Division, National Institute of Standards and Technology, Gaithersburg, Maryland 20899*
(Received 9 March 1998)

Dewetting of polystyrene films on a silicon substrate is investigated as a function of film thickness h. We observe the nucleation of holes in the early stage of dewetting for relatively thick films ($h > 100$ Å), as observed previously, but the breakup of thinner films occurs through the growth of uniformly distributed surface undulations ("spinodal dewetting"). The average amplitude δh of these undulations increases exponentially up to the film rupture point where δh becomes comparable to h, as predicted by a capillary wave instability model. [S0031-9007(98)06787-8]

PACS numbers: 68.15.+e, 47.20.–k, 68.45.–v

An understanding of the stability and homogeneity of ultrathin polymer films on solid substrates has technological and scientific importance in applications ranging from coatings, dielectric layers, and lubricant surfaces to fundamental studies of polymer diffusion or adsorption [1,2]. A number of factors influence the dewetting of polymer films, such as film thickness, polymer-surface interaction, viscosity, and surface tension. Our present study focuses on the effect of film thickness on the dewetting of polystyrene (PS) films having a thickness less than 200 Å, a range for which there has been little previous study.

A classical model of thin film breakup by Vrij [3] indicates that the capillary instability mechanism of thin film breakup by thermal fluctuations is analogous to spinodal decomposition in fluid mixtures, where *height fluctuations* in this model correspond to *composition fluctuations* in the fluid mixture. Of course, the surface energy rather than the fluid interfacial energy is the driving force for the film rupture process so this is only a mathematical analogy between these "phase separation" processes. The original Vrij model emphasized the breakup of soap films where there are two free liquid-air boundaries, and Brochard and Dalliant [4] have recently developed a variant of this model for investigating thin liquid films dewetting from solid substrates. These models predict the growth of small surface undulations $Z(x, t)$,

$$Z(x, t) = h + \delta h \exp(iqx), \qquad \delta h = \delta h_0 \exp(Rt), \quad (1)$$

with film thickness h, fluctuation amplitude δh, growth rate R, and time t. The coordinate x is taken to be parallel to the surface and q denotes wave vector. The surface undulation gives rise to a pressure gradient which drives the film instability if the effective Hamaker constant A is negative (nonwetting liquid). This film breakup mechanism is much like the hydrodynamic instability governing the late stage coarsening of phase separating fluid mixtures [5].

In the linearized capillary wave instability model [3,4], thermally induced thickness fluctuations are exponentially amplified if their wave vector is less than the critical wave vector q_c, while they decay if $q > q_c$. The fastest growing fluctuations in the linearized model, corresponding to the early stage of the dewetting process, have a time independent characteristic wave vector q_M and a growth rate R_M,

$$q_M = \sqrt{3/2}\,(a/h^2) = q_c/\sqrt{2}, \quad R_M = 3\gamma a^4/4\eta h^5, \quad (2)$$

where $a^2 = |A|/6\pi\gamma$ defines a molecular scale surface interaction parameter, γ is the surface tension, and η is the film viscosity [4]. These quantities have counterparts in the Cahn-Hilliard theory of mixture phase separation [6]. Equation (2) is compared extensively to our experiments below.

Reiter [7] and Stange [8] have examined the dewetting of relatively high molecular weight polymer thin films ($h \gtrsim 5$ nm) where the dewetting process initiates through the formation of holes of uniform diameter. Stange [8] provides some direct evidence for the growth of randomly distributed undulations in the early stage of dewetting, and Reiter observed the number density of holes scaling as $r \sim h^{-4}$ [4,7]. However, Jacobs *et al.* [9] have shown that the presence of air bubbles and other defects can lead to hole formation by heterogeneous nucleation and have questioned the existence of dewetting arising from thermally excited surface fluctuations in polymer films.

Evidence for the breakup of films by spinodal dewetting is limited. Bischoff *et al.* [10] found bicontinuous spinodal-like surface patterns in thin liquid metal films on silica substrates whose characteristic wavelength varied as h^2 [see Eq. (2)]. Buschbaum *et al.* [11a] observed the late stage of dewetting of thin polystyrene films on silicon oxide substrates and found relatively uniform droplet configurations having a size consistent with the spinodal dewetting model. Thiele *et al.* [11b] found a bimodal hole distribution in the dewetting of evaporating collagen solutions which was attributed to a combination of nucleation growth and spinodal dewetting mechanisms. All this evidence on thin film dewetting is consistent with spinodal dewetting, but there have been no kinetic studies of thin film breakup which are required to fully establish the spinodal dewetting model [3,4]. Notably, the analytic predictions of Eqs. (1) and (2) for the amplitude, lateral

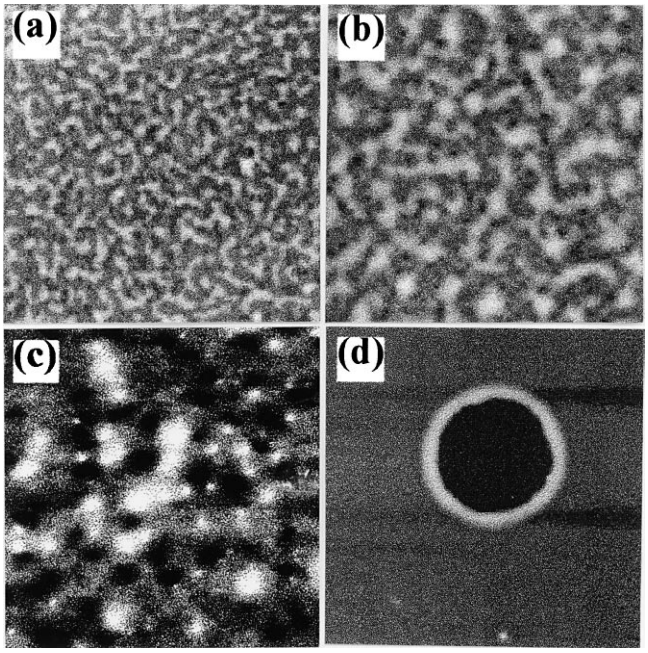

FIG. 1. AFM topogaphies showing dewetting patterns in the early stage for films with different thicknesses, but a fixed annealing temperature, 115 °C. (a) $h = 45$ Å, $t = 4$ min, 2.5×2.5 μm^2; (b) $h = 75$ Å, $t = 150$ min, 5×5 μm^2; (c) $h = 125$ Å, $t = 5.5$ h, 3.5×3.5 μm^2; (d) $h = 350$ Å, $t = 25$ h, 25×25 μm^2.

size, and rate of growth of the capillary wave undulations apply to the early stage kinetics of film breakup so that kinetic data at short times are especially important for verifying the capillary wave instability model of dewetting.

In the present work, we focus on dewetting in thin low molecular weight polymer films ($h < 100$ Å) where the initial fluctuation amplitude δh_0 is presumably more comparable to the film thickness h. The film surface undulates uniformly, creating *height variation* patterns similar to those observed for *composition variations* in near-critical composition phase separating fluid mixtures. Not only do these polymer dewetting patterns resemble the previous metallic film dewetting observations [9], but the early stage exponential growth kinetics of the undulation amplitude δh, the h dependence of q_c and q_M, the constancy of the ratio $q_c/q_M \approx \sqrt{2}$, and the estimate of the h dependence of R_M support the capillary wave model [see Eq. (2)]. A late stage droplet coalescence regime is also observed, which is the counterpart to late stage phase separation in fluid mixtures.

Our model polymer was low molecular weight ($M_w = 4000, R_g \sim 14$ Å) and monodisperse ($M_w/M_n = 1.04$) polystyrene. Uniform thin films were prepared, as demonstrated below by atomic force microscopy, AFM (TopoMetrix [12]) and x-ray reflectivity (XR) measurements (interface roughness ≤ 5 Å). The films were prepared by spin casting the PS from toluene solutions onto polished Si(100) wafers (Semiconductor Processing, Inc. [12]). The wafers were previously cleaned by placing in a 1:1 mixture of H_2SO_4/H_2O_2 (30%) at 80 °C for at least 1 h, rinsed with de-ionized water, and then placed under vacuum at room temperature for at least 24 h to remove residual solvent. Film thickness h, as measured by XR after drying, ranged from 45 to 350 Å. Samples were then annealed at 115 °C in vacuum for different times, and quenched to room temperature for AFM observations.

We first investigate the qualitative influence of varying film thickness on the dewetting process. Figure 1 shows AFM images of early stage PS films dewetting for h in the range of 45 to 350 Å after annealing at 115 °C for different times. For the thinner films ($h \leq 100$ Å) shown in Figs. 1(a), 1(b), we find a biscontinuous surface pattern, while for the thicker film ($h = 350$ Å) shown in Fig. 1(d), we see the formation of holes by a nucleation process [7,8]. At a late stage of dewetting these thicker films form droplet configurations resembling Voronoi tessellation patterns [7,8]. This is the process one usually associates with film dewetting. Figure 1(c) shows an intermediate thickness ($h = 125$ Å) where both holes and surface undulations form over a large part of the surface so this must be near the "crossover thickness" where the dewetting process changes its character. The study below focuses on the dewetting of PS films with $h \leq 100$ Å where spinodal dewetting is observed.

Figure 2 shows representative topographical AFM images of the 45 Å PS film covering a broad range of annealing times at 115 °C from 21 min to 43 h. The bicontinuous surface pattern for the early dewetting [Figs. 2(a), 2(b)] stage appears superficially similar to

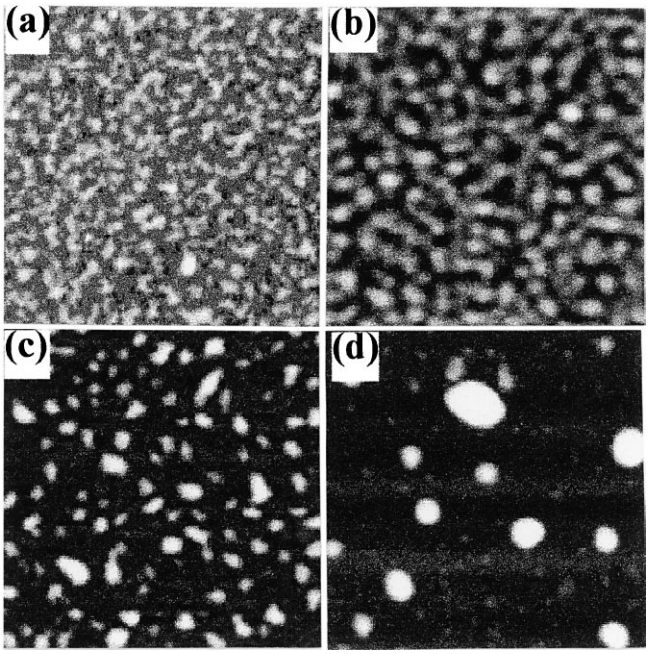

FIG. 2. AFM topographies for a PS film with thickness of 45 Å for a range of annealing times at 115 °C: (a) 21 min, (b) 90 min, (c) 7.5 h, and (d) 43 h. All image sizes (2.5×2.5 μm^2).

spinodal decomposition patterns found in phase separation measurements and simulations [6,10]. The average amplitude of the undulations grows with time, and the film eventually breaks into small, but uniformly distributed droplets. These droplets are not stable and subsequently coarsen, presumably through a coalescence process. This behavior can be contrasted to the dewetting of thicker films [see Fig. 1(d)].

In Fig. 3, we consider the early stage of the 45 Å PS thin film dewetting in more detail. The surface undulation in this stage is apparent from the AFM line profile of the film height. The lower inset of Fig. 3 is an AFM line profile of the topographic image in Fig. 2(a) after annealing at 115 °C for 21 min. These profile data allow us to estimate the average amplitude δh and the in-plane correlation length $\Lambda(t)$ of the surface undulations. $\Lambda(t)$ can be obtained from a radial average of a 2D fast Fourier transform (FFT) of the AFM topographical images. The upper right inset of Fig. 3 is a 2D FFT of Fig. 2(a), and the radial average of this FFT spinodal ring image is shown by the open circles. A peak in the scattering intensity is observed at $q = q^*$, determining the scale of the in-plane surface undulations [$\Lambda(t) \equiv 2\pi/q^*$]. In the "early stage" of dewetting, the characteristic wave vector q^* corresponds to the size of the most unstable surface undulations, $q_M = q^*$ in Fig. 3, while q^* becomes comparable to the size of the droplets following the film breakup. Figure 3 also shows a radial average profile (filled circles) for an AFM image of the same 45 Å PS film after a longer annealing time of 45 min at 115 °C. It is then possible to define a "crossover wave vector" q_c, such that the thickness fluctuations grow in amplitude for $q < q_c$, while those with $q > q_c$ decrease with time. The ratio of the two characteristic scales shown in Fig. 3 equals $q_c/q_M = 1.37$, which accords well with the theoretical estimate [4], $q_c/q_M = \sqrt{2} \cong 1.41$.

The evolution of the surface undulations can be monitored through measurement of $\delta h(t)$ and $q^*(t)$ over a range of annealing times t. Figure 4(a) shows that δh grows exponentially in the initial stage of dewetting (up to 90 min), in accord with the predictions of the spinodal dewetting model [3,4] [see Eq. (1)]. A slowing down from exponential growth occurs when $\delta h \approx 12$ Å, corresponding to an annealing time of about 90 min. This deviation from an exponential growth occurs when the total average height variation $2\delta h$ approaches half the film thickness, $2\delta h \geq 24$ Å $\approx h/2$. However, the film does not rupture into droplets until $2\delta h$ becomes nearly equal to the film thickness, $2\delta h$ (180 min) ≈ 40 Å $=$ 0.9 h, which is consistent with a general rupture criterion for the breakup of liquid films and threads into droplets [3,4,13].

A plot of $\log q^*$ versus $\log t$ [Fig. 4(b)] suggests two distinct stages of the spinodal dewetting process. In the first 90 min (early stage), q^* varies slowly with time, much like the early stage of spinodal decomposition in blends [14]. In the "late stage," following film breakup into droplets, the surface structure coarsens rapidly and

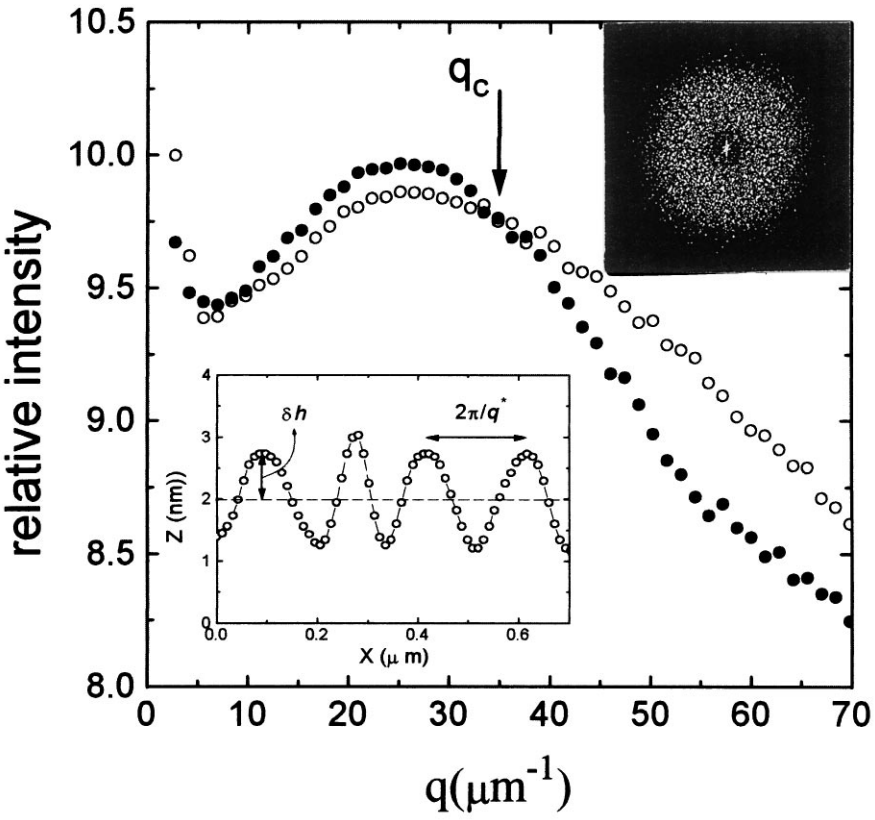

FIG. 3. Plot of relative intensity versus wave vector q. Intensity plot obtained from radial average of 2D FFT image shown in right inset. Left inset shows a typical cross-sectional profile of surface undulations taken from the data shown in Fig. 2(a). Relative intensity data at other times in the early stage of dewetting (not shown) also cross at q_c.

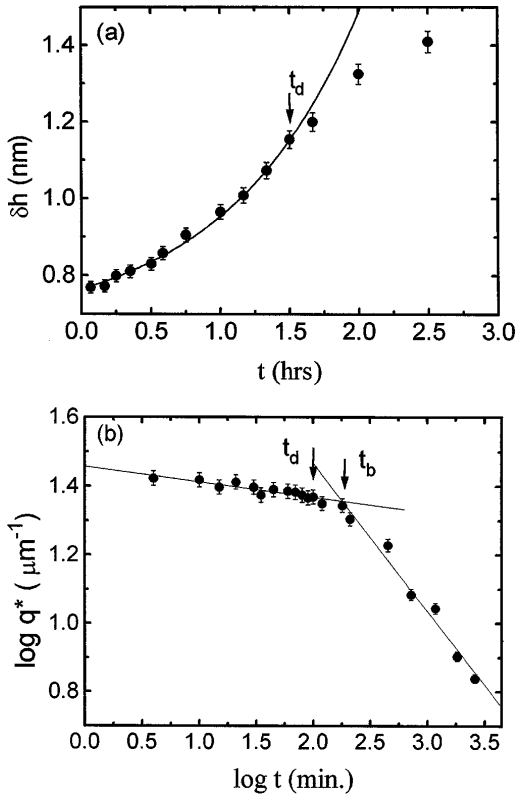

FIG. 4. (a) Plot of average amplitude δh as a function of annealing time for the 45 Å PS film. The line is an exponential fit to the early stage data and t_d denotes the deviation time where the film rupturing process begins. (b) Log-log plot of q^* vs time showing a two-stage film breakup process. The late stage regime starts at the breakup time t_b when δh approaches the film thickness (see text).

this growth can be described by an apparent power law with an exponent near -0.43. This exponent estimate is notably similar to that obtained for polymer phase separation in ultrathin blend films [15].

The linearized "spinodal dewetting" model further predicts that $\Lambda(t)$ depends quadratically on film thickness, $\Lambda \sim h^2$. Indeed, the surface pattern scale in the early stages of dewetting tends to be much larger in thicker films [see Figs. 1(a) and 1(b)], and slowly varying in time. An analysis of the radially averaged Fourier transforms of early stage dewetting patterns gives a ratio $\Lambda_{45}/\Lambda_{75} \cong q_{M,75}/q_{M,45} = 0.36$, which is compared to the spinodal dewetting model prediction of 0.36 from Eq. (2).

The growth rate R_M of the spinodal dewetting process is also expected to depend strongly on film thickness [see Eq. (2)]. A fit of the data shown in Fig. 4(a) indicates that the average initial height amplitude in the 45 Å film, $\delta h_0 \approx 7.7$ Å, and the reciprocal of the coarsening rate equals $1/R_{M,45} = 198$ min. Inserting literature parameter values [16] for PS ($h = 45$ Å, $\gamma = 31.9$ mN/m, $\eta = 2.25 \times 10^4$ Pa · s, and $A = -7.42 \times 10^{-20}$ J) into Eq. (2) gives $1/R_{M,45} = 194$ min. As both the 75 and 45 Å films are annealed at the same temperature, it seems reasonable to assume that δh_0 is the same for both the 75 and 45 Å films (δh_0 describes the amplitude of equilibrium capillary waves, which has a weak dependence on film thickness [17], so that the δh_0 values should be nearly equal in these films). Utilizing the assumed value $\delta h_0 \approx 7.7$ Å and a single δh measurement for the 75 Å film in the exponential growth regime allows us to make a preliminary estimate $1/R_{M,75} = 2509$ min, a much faster rate. The relative rate estimate $R_{M,45}/R_{M,75} \approx 12.7$ is consistent with the theoretical prediction of 12.9 from Eq. (2).

Our measurements show a transition in the qualitative nature of the dewetting process in PS films with $h < 100$ Å. It is emphasized that the polymer molecular weight employed in our study is low and that viscoelastic effects associated with higher molecular weights could have a significant impact on the dewetting process, perhaps even suppressing the effect entirely. Future work should contrast the dewetting of entangled and unentangled thin ($h < 100$ Å) polymer films, and the temperature varied to determine if there is a crossover between nucleation and spinodal dewetting in films of fixed thickness.

We acknowledge support of the work by the Polymer Program of the National Science Foundation (Grant No. DMR 9712194) and useful discussions with Holger Gruell, Eric Amis, and Michael Moldover.

*Corresponding author.

[1] T. P. Russell, Mater. Sci. Rep. **5**, 171 (1990).
[2] R. A. L. Jones *et al.*, Europhys. Lett. **12**, 41 (1990).
[3] A. Vrij, Discuss. Faraday Soc. **42**, 23 (1966); A. Vrij and J. Th. G. Overbeek, J. Am. Chem. Soc. **90**, 3074 (1968).
[4] (a) F. Brochard and J. Daillant, Can. J. Phys. **68**, 1084 (1990); (b) A. Milchev and K. Binder, J. Chem. Phys. **106**, 1978 (1997). This work presents Monte Carlo simulations supporting the existence of spinodal dewetting.
[5] E. D. Siggia, Phys. Rev. A **20**, 595 (1979).
[6] S. C. Glotzer, Ann. Rev. Comp. Phys. **2**, 1 (1995).
[7] G. Reiter, Phys. Rev. Lett. **68**, 75 (1992); Langmuir **9**, 1344 (1993); Macromolecules **27**, 3046 (1994).
[8] T. G. Stange and D. F. Evans, Langmuir **13**, 4459 (1997).
[9] K. Jacobs *et al.*, Langmuir **14**, 965 (1998).
[10] J. Bischof *et al.*, Phys. Rev. Lett. **77**, 1536 (1996).
[11] (a) P. Muller Buschbaum *et al.*, Europhys. Lett. **40**, 655 (1997); (b) U. Thiele *et al.*, Phys. Rev. Lett. **80**, 2869 (1996).
[12] The reference to commercial equipment does not imply its recommendation or endorsement by the National Institute of Standards and Technology.
[13] T. Mikami *et al.*, Int. J. Multiphase Flow **2**, 113–138 (1975).
[14] M. Motowoka *et al.*, J. Chem. Phys. **99**, 2095 (1993); C. C. Han and A. Z. Akcasu, Annu. Rev. Phys. Chem. **43**, 2095 (1992).
[15] L. Sung *et al.*, Phys. Rev. Lett. **76**, 4368 (1996); B. Ermi *et al.*, J. Polym. Sci. B **36**, 191 (1998).
[16] S. Wu, in *Polymer Handbook*, edited by J. Brandup and E. H. Immergut (Wiley, New York, 1989); T. G. Fox and P. J. Flory, J. Polym. Sci. **14**, 315 (1954); A. Sharma and G. Reiter, J. Colloid Interface Sci. **178**, 383 (1996).
[17] M. Sferrazza *et al.*, Phys. Rev. Lett. **78**, 3693 (1997).